This is a repository copy of *High-fidelity CFD simulations of pulsed sieve-plate extraction columns*.

White Rose Research Online URL for this paper:
http://eprints.whiterose.ac.uk/105537/

Version: Accepted Version

High-fidelity CFD simulations of pulsed sieve-plate extraction columns

Z. Khatir*, B.C. Hanson, M. Fairweather and P.J. Heggs

School of Chemical and Process Engineering, University of Leeds, Leeds LS2 9JT, UK

*Email: z.khatir@leeds.ac.uk

Abstract

The pulsed sieve-plate extraction column (PSEC) is a technology for liquid-liquid extraction processes widely used in various industries, and commonly employed in nuclear fuel reprocessing. A high fidelity computational fluid dynamic model of a solvent PSEC has been developed and run with single-phase water. The PSEC investigated consists of two perforated plate internals, operated under 1 Hz pulsing frequency, 20 mm amplitude and a plate spacing of 50 mm. The CFD used was based on unsteady flow calculations undertaken with a conventionally used RANS model, closed with the standard k-ε turbulence model, and a large eddy simulation (LES). Results are compared with experimental data, where available, and agreement is improved by using the more accurate predictions of the turbulent flow in the column offered by large eddy simulation. Significant differences between predictions of the RANS and LES approaches are also found, drawing into question the usefulness of the former for predicting these complex flows. The CFD analysis brings useful insight into the hydrodynamics in PSECs, which provides better understanding for further work on both single- and two-phase flows in these devices.

1   Introduction

Liquid-liquid extraction processes are widely used in various industries such as the food and minerals industry, in oil and gas operations, and in the nuclear industry. Pulsed sieve-plate extraction columns are crucial in nuclear spent fuel reprocessing to separate reusable elements, such as uranium and plutonium, from the other waste fuel components, which are handled as radioactive wastes. Like other equipment dedicated to liquid-liquid extraction processes, PSECs are utilised to achieve high interfacial area between the two liquids, by allowing the efficient breakage of the dispersed phase. Van Dijck (1935) subsequently suggested that the volumetric efficiency of a perforated plate could be improved by either pulsing the liquids or reciprocating the plates.

Understanding the flow characteristics of PSECs is crucial to process design and optimization. In this context, computational engineering science, the technology that deals with the development and application of computational models and simulations coupled with high performance computing to solve complex physical problems arising in engineering analysis and design, is a powerful tool, complementary to experiments. In this work we apply this approach to study and predict a PSEC's flow characteristics.

A PSEC consists of a vertical, cylindrical tube containing a set number of stationary, horizontal, perforated plates, as shown schematically in Figure 1. The two immiscible liquids are added at the opposite ends of the column - the low density liquid is added at the bottom and the heavy one at the top. Gravity provides the motive force, with the heavier phase falling to the bottom of the column whilst the lighter phase rises to the top. The pulsing action provides agitation to break-up the light phase and disperse it, as well as forcing it upwards. Plate spacing is designed to replicate the equivalent of a separation stage in a mixer settler, and the hole size in the plates, together with the pulse frequency and amplitude, determines the droplet size. The complexity of the system makes it difficult to define the mass transfer coefficient using correlations similar to those that exist for mixer settlers.
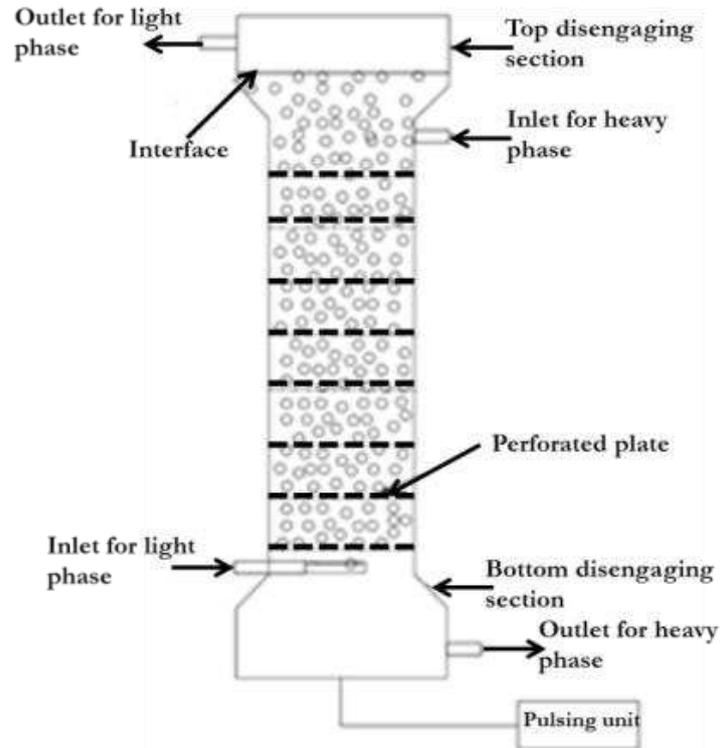
Figure 1: Diagram showing the internal workings of a typical pulsed plate column.

A recent review of empirical correlations derived from experiments found little agreement on an overall correlation, leaving the engineer relying on proving any design via pilot plant trials (Yadav and Patwardhan, 2008). Designers of full scale plant are thus left with the issue of a paucity of design rules to size and define an appropriate unit. Hence the provision of reliable computational tools for predicting these devices, and ultimately optimizing their design, is a pressing need for industry.

2   CFD modelling and solution strategy

In the present work, a two-plate PSEC CFD-based generic model is developed, as shown in Figure 2, embedding geometric and operating design variables such as hole size d, column diameter D, perforated plate spacing h, and appropriate boundary conditions. A simple design was initially chosen to assess the feasibility of applying CFD-based approaches to this problem, and in the interests of computational efficiency.
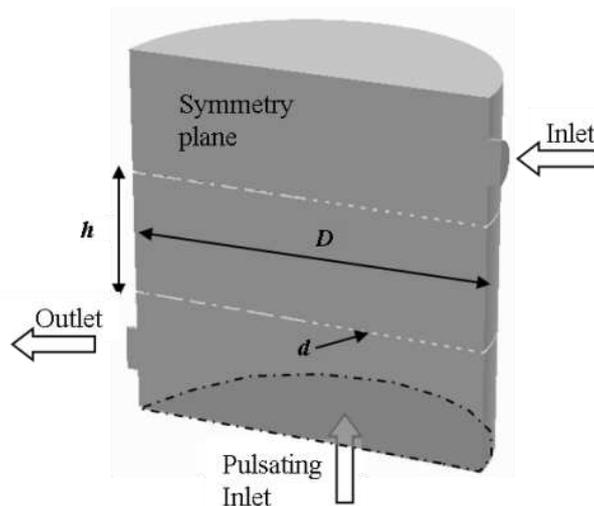
Figure 2: Two-plate PSEC generic model as a function of hole size d, column diameter D and perforated plate spacing h, with appropriate boundary conditions.

Table 1 contains the precise details and dimensions of the geometry used in the CFD simulations. These were selected for the investigation as they are representative of typical columns found in operating fuel reprocessing plants in the UK and France.

Table 1: Dimensions and geometry of the PESC.

Parameter	Dimension
Column diameter, D (m)	0.150
Hole diameter, d (m)	0.003
Plate spacing, h (m)	0.50
Plate thickness, t (m)	0.001
Column height, H (m)	0.152
Fractional open area, e	23 %
Number of holes, N_h	575
Number of perforated plates, N_p	2

In the present work, a single-phase flow of water at 25ºC was employed as the working fluid within the computational domain. Investigation of a single-phase flow alone was undertaken at this stage to allow further understanding of the flow characteristics and operation of PSESs to be established, prior to subsequently moving to two-phase flow. The OpenFOAM CFD toolbox was used for the calculations (OpenFOAM Foundation Ltd, 2016).

Unlike previous work (Yadav and Patwardhan, 2009; Amokrane et al , 2014), unsteady flow calculations were undertaken using a k-ε turbulence model (Launder and Spalding, 1972) based RANS approach and a large eddy simulation which employed a one-equation subgrid-scale model (Schumann, 1975). Indeed, the only previous applications of CFD to this flow geometry have employed models of the former type, and in this work LES is used as a benchmark against which simpler RANS approaches can be assessed. No-slip boundary conditions were imposed at column walls and on the internal plates, whereas the velocity inlet and pressure outlet boundary conditions were imposed as shown in Figure 2. Water entered the column with a velocity $U_{in} = 0.086$ m s^{-1} and the consequential superficial velocity was $U_s = 0.00124$ m s^{-1}. The velocity inlet condition was prescribed at the bottom of the column, defining a sinusoidal pulse as employed by Yadav and Patwardhan (2009) for single-phase flow as:

$$U_p = Af \sin(2\pi ft) \qquad\qquad (1)$$

with A = 0.02 m and f = 1 Hz.

The Open Source OpenSCAD and NETGEN tools were used to generate the geometry and grid, respectively. This resulted in 0.52M unstructured tetrahedral mesh elements with a finer mesh size near the plates, as illustrated in Figure 3.
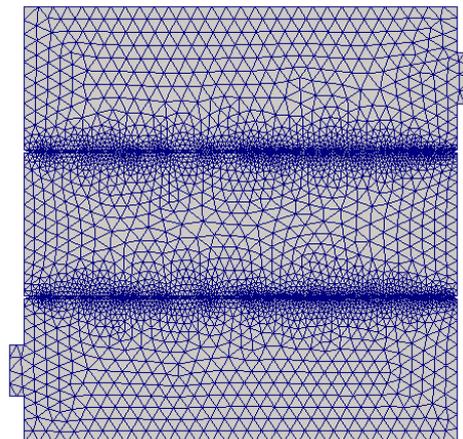
Figure 3: PSEC mesh employed in the simulations.

For validation purposes, the following empirical equation for the axial dispersion in PSECs, obtained by Ingham et al. (1995) at zero flow rate, was used:

$$D_{ea}^0 = a \left(\frac{\rho d f A}{\mu}\right)^{-0.3} (fA)(1-e^2)\frac{D^{1.33}}{(he^2 C_D^2)^{0.33}} + \qquad b\left(\frac{fA^2}{e^2}\right)\left(\frac{h}{A}\right)^{0.45} \qquad (2)$$

where D_{ea}^0 is the axial dispersion coefficient at zero flow rate that is only caused by pulsation. The factors a and b are empirical constants for the effects of axial mixing close to the plates and in the main domain of the column compartments, respectively, whose values are given for different geometries by Ingham et al. (1995). Lastly, C_D is the drag coefficient in the plate holes, taken to be equal to 0.6.

Based on a theoretical analysis, the influence of the continuous phase velocity is given by the formulation proposed by Miyauchi and Oya (1965):

$$D_{ea} = D_{ea}^0 \left(1 + \frac{u}{2fA}\right) \qquad (3)$$

3   Results and discussion

The key parameter of the operating PSEC are the drop size and overall dispersion, as these are the main driving force behind the mass transfer between the two phases.

Predicted coefficients of dispersion were found to be 1.3×10^{-3} and 6.72×10^{-4} m^2 s^{-1} from the k-ε and LES computations, respectively, and these values are in reasonable agreement with that of 2.2×10^{-4} m^2 s^{-1} obtained using Eq. (2). They are also in the range 10^{-4} to 10^{-3} obtained by Ingham et al. (1995), with the LES prediction being of superior accuracy to that obtained using the RANS model.

In the following, times t = 0.25 and t = 0.75 denote instants when U_p = A and U_p = -A, respectively, whereas times t = 0.5 and t = 1 occur at U_p = 0, during down stroke and upstroke, respectively.
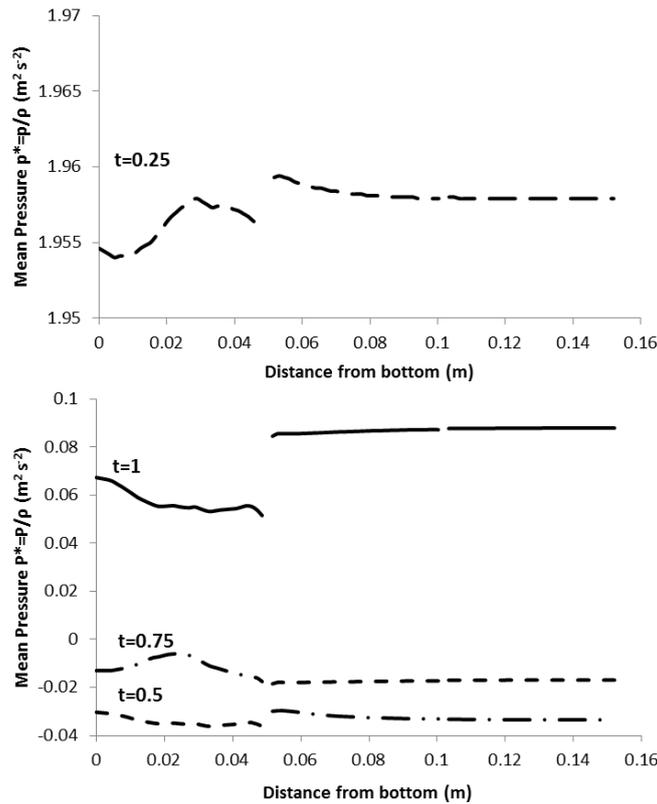
Figure 4: Mean average pressure, P*=P/ρ, along thecentreline at various times for the k-ε simulation.

As displayed in Figures 4 and 5, the mean average pressure along the centreline of the column clearly emphasizes a high-pressure zone at t = 0.25, when U_p is at its maximum, that is predicted by both approaches. Fluctuations are noticeable between the bottom of the column and plate 1 (i.e. located at z = 0.05m), whereas the pressure is constant from z = 0.05m upwards in both sets of predictions. The LES pressure prediction is 10% to 33% higher than the k-ε prediction. This is also true at the other times

considered in these figures, with both approaches capturing the negative pressures found at t = 0.5 and t = 0.75, and both sets of predictions being in qualitative, if not quantitative, agreement.

Unlike conventional k-ε turbulence model based RANS approaches, particularly for the complex flows considered herein, the LES approach is better suited to predicting the hydrodynamic behaviour in the PSEC owing to its ability to capture the small turbulent eddy flow structures. This is clearly evidenced in Figure 6 where the mean average velocity field on the y-symmetry plane of the PSEC is shown at times t = 0.25, t = 0.5, t = 0.75 and t = 1 for both the RANS and LES simulations.
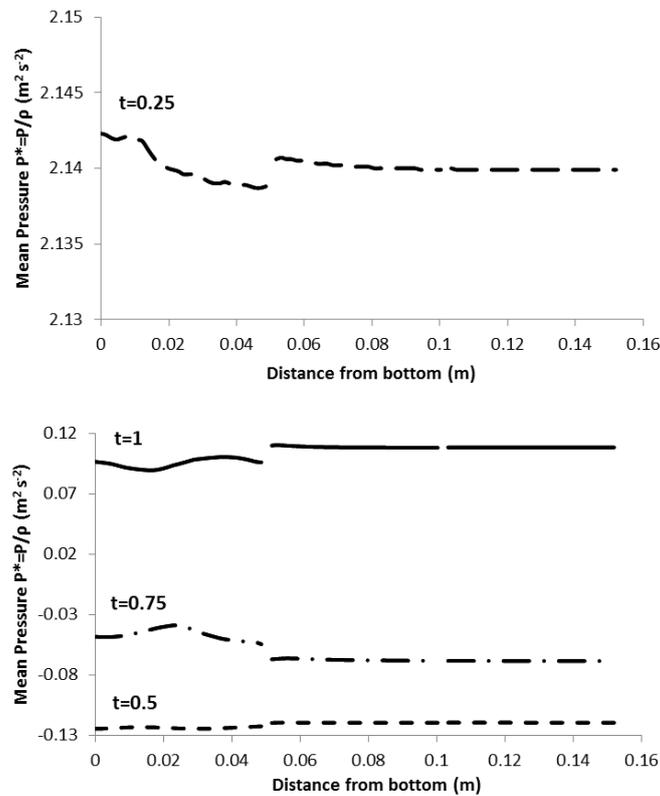
Figure 5: Mean average pressure, $P^*=P/\rho$, along the centreline at various times for LES.

The results show jet flow through the holes in the plates allowing efficient mixing of the flow, which is an important feature for an effective PSEC, also shown in Figure 6. There are clear differences between the two sets of predictions, especially at times t = 0.5 and t = 1 when U_p = 0 during the down stroke and upstroke, respectively. These results emphasize the ability of LES to capture such features which are less well resolved by the RANS model.

This shortcoming of the k-ε based RANS approach is further demonstrated in Figure 7. Here, the mean turbulence kinetic energy and velocity vector field on the y-symmetry plane are shown at times t = 0.5 and t = 1 for both sets of predictions. Equivalent results for the mean turbulence kinetic energy dissipation rate are given in Figure 8. The LES is seen to provide much greater detail than the RANS based approach, with detailed vortical structure and recirculation zones clearly visible for the LES. Considering the results of Figures 6 to 8 as a whole, the pulsed flow generates vortices in the flow field which are clearly distinct at times t = 0.5 and t = 1. These vortical structures produce the shear rate necessary to disperse the liquid phase in any two-phase flow, as well was the droplet coalescence necessary for mass transfer (Bujalski et al., 2006), with the turbulence energy dissipation rate, ε, given in Figure 8 directly related to the shear rate.
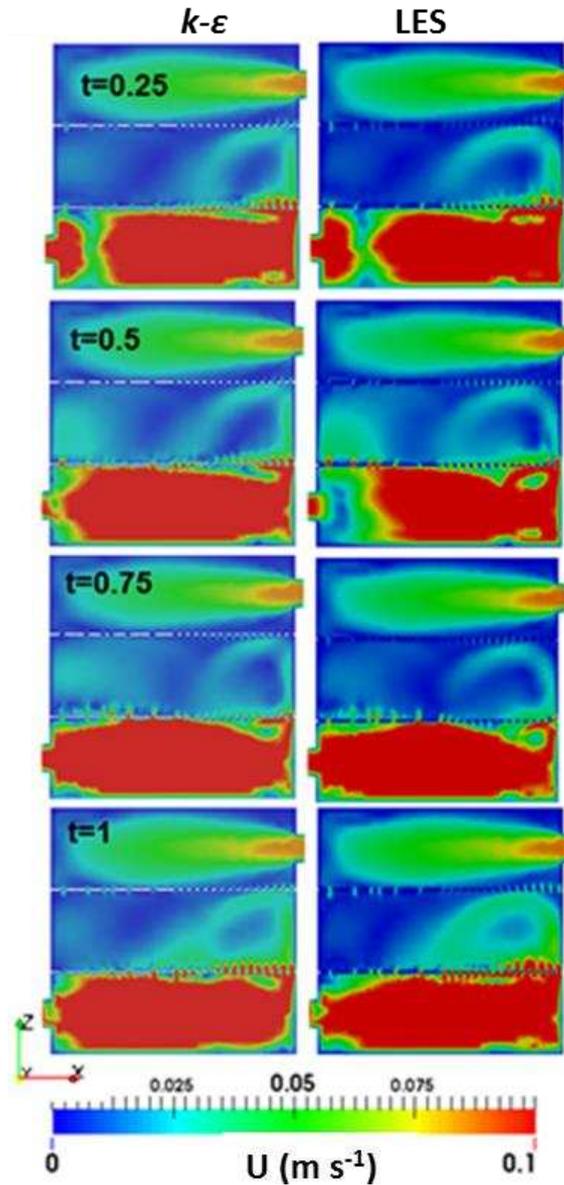
Figure 6: Mean average velocity field on the y-symmetry plane at times t = 0.25,
t = 0.5, t = 0.75 and t = 1 for the RANS and LES computations.

Previous studies (Hafez and Baird, 1978; Kumar and Hartland, 1996) have shown that the specific energy dissipation rate due to mechanical agitation can be estimated from the following relationship:

$$\varepsilon = \frac{2\pi^2\,(1-e^2)}{3h\,C_D\,e^2}(Af)^3 \qquad (4)$$

where the value of the discharge coefficient, C_D, is assumed to be 0.6 as in Eq. (2).
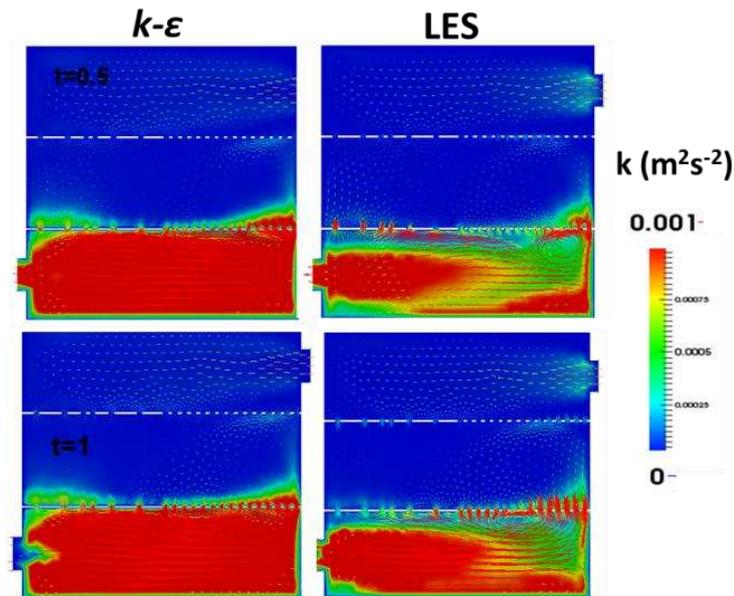
Figure 7: Mean turbulence kinetic energy and velocity vector field on the y-symmetry plane at times t = 0.5 and t = 1 for the RANS and LES computations.
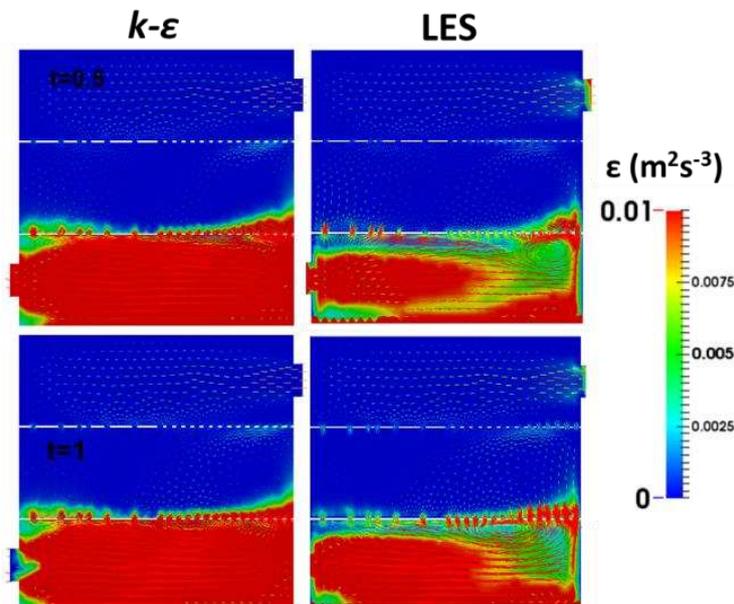
Figure 8: Mean turbulence kinetic energy dissipation rate and velocity vector field on the y-symmetry plane at times t = 0.5 and t = 1 for the RANS and LES computations.

The value of the average energy dissipation rate for the system considered given by Eq. (4) is 0.42 $m^2 s^{-3}$, whilst the CFD predictions of ε are 0.006 $m^2 s^{-3}$ from both the RANS and LES computations. It should be noted, however, that the average energy dissipation in a PSEC might not represent adequately the average level of turbulence and mixing during operation, and may thus be only a crude approximation (Bujalski et al., 2006). For instance, in the system considered, the maximum value of the average predicted ε was 4.4, 2.1, 2.2 and 2.3 $m^2 s^{-3}$ for the RANS model, and 58.7, 6.4, 20.0 and 3.4 $m^2 s^{-3}$ for the LES, at times t = 0.25, 0.5, 0.75 and 1, respectively. Given the greater accuracy of LES, these results indicate that RANS using k-ε turbulence modelling significantly under predicts the turbulence properties. However, the question remains whether the maximum turbulence energy dissipation occurs at a point in the pulsation cycle and at a location in the PSEC where energy can be used effectively to allow proper phase dispersion.

Another way to examine the flow behaviour of such complex turbulent flow systems is to use the second invariant of the velocity gradient tensor Q defined as (Hunt et al., 1988; Haller, 2005):

$$Q = \frac{1}{2}[|\boldsymbol{\Omega}|^2 - |\boldsymbol{S}|^2] \hspace{3cm} (5)$$

where $\boldsymbol{S} = \frac{1}{2}[\nabla v + (\nabla v)^T]$ and $\boldsymbol{\Omega} = \frac{1}{2}[\nabla v - (\nabla v)^T]$ are the rate-of-strain tensor and the vorticity tensor, respectively.
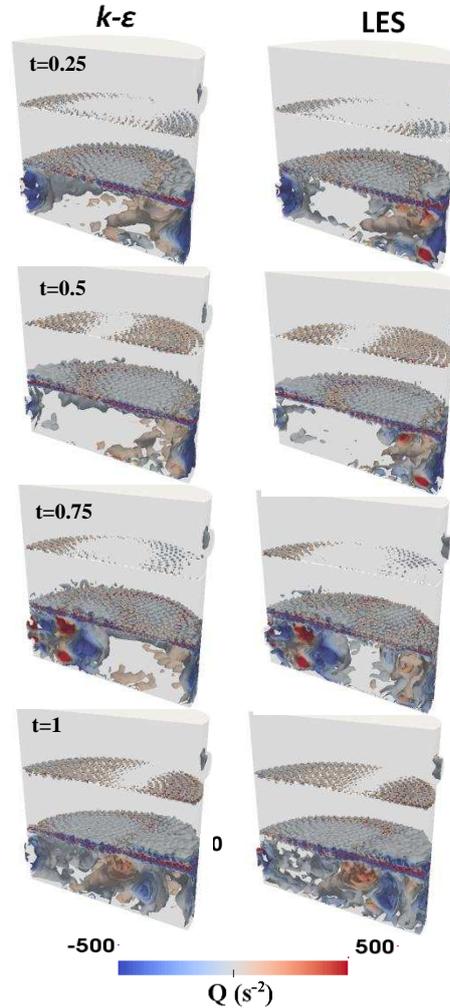
Figure 9: Second invariant of the velocity gradient tensor Q at times t = 0.25, t = 0.5, t = 0.75 and t = 1 for the RANS and LES computations.

Figure 9 displays the isosurface of Q at times t = 0.25, 0.5, 0.75 and 1 for the RANS and LES computations. The small eddy flow structures are visible in both the RANS and LES predictions near the plates. Three-dimensional effects are also clearly identifiable, and a wave structure is noticeable on top of plate 2 (i.e. located at z = 0.102m) as well as on top of plate 1 (at z = 0.05m).

This wave seems to follow the pulsating inlet U_p as described in Figure 2. It travels from left to right and spreads in the spanwise direction in a very complex manner until it reaches the walls. It then moves down the column, entraining flow and growing, hence generating larger vortical structures and recirculation zones, as depicted in Figures 6 to 8. The LES results also show small eddies below plate 1 at t = 0.5 and t = 1. The RANS simulation does not capture these small eddy flow structures.

The detailed and realistic description of the flow hydrodynamics and characteristics of PSECs is a necessary step towards an accurate prediction of their performance and ultimately their design optimisation, which will be the subject of future work. This will embed surrogate-modelling approaches, a methodology that has been successfully applied by the authors for a range of engineering applications (e.g. the design optimisation of energy efficient material and commercial ovens (Khatir et al., 2015, 2016)), as well as full CFD computations into an optimisation framework.

4   Conclusions

A high-fidelity CFD-based methodology has been developed to analyse and characterise single-phase flow patterns present, due to oscillation, in an idealised but representative pulsed sieve-plate extraction column, and is demonstrated to be an effective tool to investigate such complex flow systems. The models examined were RANS based, closed using a k-ε turbulence model, and a large eddy simulation. Previous investigations of PSECs have only used the former approach, whilst the present work demonstrates that this is clearly inadequate given the complexity of the flows involved, with significant differences occurring between predictions of the two approaches. Future work will consider a CFD-based design optimization framework to improve the efficiency of PSECs though improved design. Experimental data is also currently being gathered for use in the validation of models of the type described herein.

Acknowledgements

References

Amokrane, A., Charton, S., Lamadie, F., Paisant, J.F. and Puel F. (2014), Single-phase flow in pulsed columns, Chem. Eng. Sci., Vol. 114, pp. 40-50.

Bujalski, J.M., Yang, W., Nikolov, J., Solnordal, C.B. and Schwarz, M.P. (2006), Measurement and CFD simulation of single-phase flow in solvent extraction pulsed column, Chem. Eng. Sci., Vol. 61 pp. 2930-2938.

Hafez, M.M. and Baird, M.H.I. (1978), Power consumption in a reciprocating plate column, Chem. Eng. J., Vol. 9, pp. 229-238.

Haller, G. (2005), An objective dentition of a vortex J. Fluid Mech., Vol. 525, pp. 1-26.

Hunt J.C.R., Wray, A.A. and Moin, P. (1988), Eddies, streams, and convergence zones in turbulent flows, Center for Turbulence Research, Report CTR-S88, pp. 193-208.

Ingham, J., Slater, M.J. and Retamales J. (1995), Single phase axial mixing studies in pulsed sieve plate liquid-liquid extraction columns, Trans. IChemE, Vol. 73, pp. 492-496.

Khatir, Z., Taherkhani, A.R., Paton, J.B., Thompson, H.M., Kapur, N. and Toropov, V.V. (2015), Energy thermal management in commercial bread-baking using a multi-objective optimisation framework, Appl. Therm. Eng., Vol. 80, pp. 141-149.

Khatir, Z., Kubiak, K.J., Jimack, P.K. and Mathia, T.G. (2016), Dropwise condensation heat transfer process optimisation on superhydrophobic surfaces using a multi-disciplinary approach, Appl. Therm. Eng, Vol. 106, pp. 1337-1344.

Kumar, A. and Hartland, S. (1996) Unified correlations for the predictions of drop size in liquid-liquid extraction columns, Ind. Eng. Chem. Res., Vol. 35, pp. 2682-2695.

Launder, B.E. and Spalding, D.B. (1972), Mathematical models of turbulence, Academic Press Inc, London.

Miyauchi, T. and Oya, H. (1965), Longitudinal dispersion in pulsed perforated-plate columns, AIChE J. Vol. 11, pp. 395-402.

OpenFOAM Foundation Ltd., Free and Open Source CFD, website: http://www.openfoam.org, accessed 12-07-2016.

Schumann, U. (1975), Subgrid scale model for finite difference simulations of turbulent flows in plane channels and annuli, J. Comput. Phys., Vol. 18, pp. 376-404.

Van Dijck, W.J.D. (1935), Process and apparatus for intimately contacting fluids, US patent number 2011186.

Yadav, R.L and Patwardhan, A.W. (2008), Design aspects of pulsed sieve plate columns, Chem. Eng. J., Vol. 138, pp. 389-415.

Yadav, R.L and Patwardhan, A.W. (2009), CFD modelling of sieve and pulsed-sieve plate extraction columns, Chem. Eng. Res., Vol. 87, pp. 25-35.